17th World Conference on Earthquake Engineering, 17WCEE
Sendai, Japan - September 13th to 18th 2020

LATERAL COUPLING OF RECTANGULAR FIBER-REINFORCED ELASTOMERIC ISOLATORS

N. C. Van Engelen[(1)], H. Sheikh[(2)], R. Ruparathna[(3)]

[(1)] *Assistant Professor, Department of Civil and Environmental Engineering, University of Windsor, niel.vanengelen@uwindsor.ca*
[(2)] *Ph.D. Student, Department of Civil and Environmental Engineering, University of Windsor, hediyeh.sheikh@gmail.com*
[(3)] *Assistant Professor, Department of Civil and Environmental Engineering, University of Windsor, rajeev.ruparathna@uwindsor.ca*

Abstract

Reinforced elastomeric bearings are composites composed of alternating plan horizontal layers of elastomer and reinforcement. Elastomers are ideal for application as base isolators due to their ability to accommodate large recoverable strains. The formation of a composite with reinforcement, either steel or fibers, takes advantage of the near incompressibility of the elastomer to enhance the vertical and bending properties of the bearing. The result is a device that has a large vertical and rotational stiffness yet is very flexible in the lateral direction; ideal for application as a base isolator. Traditionally, steel is the reinforcement of choice. More recently, the use of fiber reinforcement has become an attractive alternative to the traditional approach. The impetus for using fiber reinforcement originates from the development of a low-cost base isolation device appropriate for widespread application, particularly in developing countries. Although the conceptual design of a fiber-reinforced and steel-reinforced elastomeric bearing is similar, the lack of flexural rigidity of the fiber reinforcement results in unique performance characteristics, especially in the lateral direction. In this paper, the lateral coupling of rectangular unbonded fiber-reinforced elastomeric isolators (U-FREIs) is investigated. Most experimental programs on elastomeric bearings are based on a two degree of freedom system where a vertical load and lateral displacements are applied. Herein, an experimental program is undertaken using an apparatus with six degrees of freedom. A vertical load is applied with simultaneous displacements applied in both primary lateral directions. The U-FREI specimen was subjected to cyclic lateral displacements including with initial lateral offsets in the secondary lateral direction, in directions angled off the principal lateral axis, and in circular motion. This experimental program is the first to investigate lateral coupling in rectangular U-FREIs. The results are presented and discussed identifying potential limitations and design considerations for coupling in the two principal lateral directions of U-FREIs.

Keywords: seismic isolation; elastomeric isolator; fiber reinforced; unbonded; lateral coupling

1. Introduction

In the past several decades, base isolation has become a common method to reduce the vulnerability of structures in many areas with medium-to-high seismic hazards [1]. The interest in seismic isolation has led to the development of fiber-reinforced elastomeric isolators (FREIs) as a potential low-cost alternative to conventional steel-reinforced elastomeric isolators (SREIs) [2]. The use of carbon fiber, or other high strength fibers, instead of steel plates was proposed in 1999 [3] to reduce the weight of the isolators and simplify the manufacturing process. Despite similarities between SREIs and FREIs, the state-of-knowledge regarding SREIs cannot completely be transfer to FREIs due to the difference in reinforcement thickness and mechanical properties.

Isolators can be placed bonded or unbonded between the upper and lower supports of the structure as illustrated in Fig. 1. SREIs are often bonded, which requires the use of thick steel end plates to mechanically fasten the isolator to the upper and lower supports. However, it is common to investigate FREIs as an un-bonded isolator which aligns with the light-weight, low-cost intention of FREIs. Studies have shown that unbonded FREIs are more effective in seismic isolation as compared with bonded FREIs [4–6]. In unbonded FREIs, a unique rollover deformation in the end sections occurs with lateral displacement due to the lack of bending rigidity of the fiber reinforcement and unbonded application [7]. This mechanism prevents the development of high tensile stresses in the end sections in comparison with identical bonded FREIs or similar bonded SREIs. This unique rollover deformation, increases the efficiency of the isolator by providing increased lateral flexibility, thereby further shifting the fundamental period of the isolated structure [4].

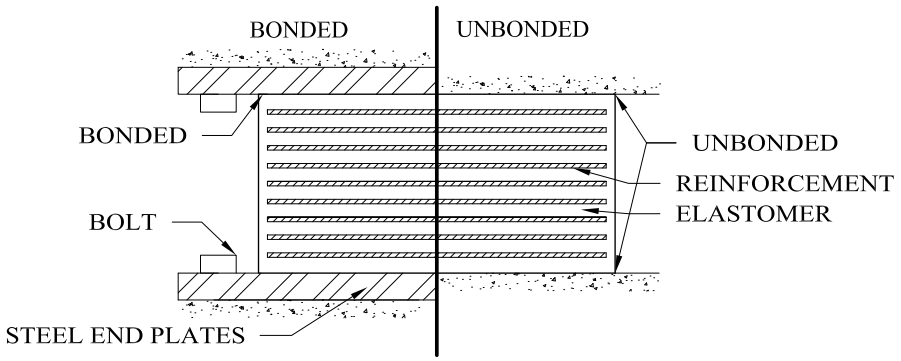

Fig. 1 - Illustration of a bonded FREI and an Unbonded FREI

Conventionally, SREIs are manufactured in symmetric shapes. The majority of theoretical and experimental programs have been conducted on the properties of circular and square specimens (particularly for seismic applications). However, FREIs can be cut to desired shape and size with the purpose of cost-saving, enhancing performance characteristics, or to address project limitations. The use of rectangular isolators, or long strip isolators, could be beneficial to provide uniform support along shear walls, thus reducing the load transfer requirements to smaller isolators [3]. Unlike bonded isolators, the critical properties of FREIs (e.g. stiffness and damping) can vary significantly in different lateral directions due to the rollover deformation.

In this paper, experimental testing is conducted to investigate lateral coupling in rectangular U-FREIs. The impact of direction of loading has been investigated in varying capacities for unbonded square FREIs [5,8–11]. However, the effect of lateral coupling in a rectangular specimen is, to the authors' best knowledge, evaluated for the first time in this study. An apparatus with six degrees of freedom was used to apply a vertical load with simultaneous displacement in both primary lateral directions. Whereas, previous experimental programs are mostly based on a two degree of freedom analysis. The isolator was subjected to cyclic lateral displacements in the form of two simultaneous displacements that offset from the principal axis and in a circular motion. The findings present potential limitations and design-related considerations for coupling in the two principal directions of a rectangular U-FREI.

2. Background

2.1 FREIs

A reinforced-elastomeric bearing is composed of alternating horizontal layers of reinforcement and elastomer (see Fig. 1). The composite action that forms between the reinforcement and elastomer results in a device that has a high vertical stiffness and low lateral stiffness; which is ideal for seismic isolation applications [12]. The primary requirement for the reinforcement is that it retains a high in-plane stiffness which provides a restraint on the elastomer as it displaces laterally due to Poisson's effect under the application of the vertical load. Traditionally, steel reinforcement was the material of choice and SREIs are one of the most widely used isolation devices to-date. By comparison, to the authors' best knowledge, FREIs have only been applied to a very small number of structures (e.g. a two-storey prototype masonry building in Tawang, India [13]) although the application is expected to increase into the future.

The use of fiber-reinforcement in elastomeric bearings dates back over 40 years ago (e.g. [14]); although Kelly [3] first proposed the use of fiber-reinforcement for seismic isolation applications and provided a framework for theoretical analysis of this type of isolator. FREIs have been enabled by the continual development of high-quality fiber materials (e.g. glass and carbon fibers). The impetus for the development of FREIs was to reduce the cost and weight of SREIs to develop a device appropriate for widespread application, particularly in developing countries where the devastation due to earthquakes is often more severe. However, subsequent investigations identified that FREIs have several advantages over conventional SREIs including adaptive characteristics [15–17] and the potential for improved energy dissipation [17–21]. Such advantages have allowed for interest in the device to extend beyond low-cost applications to a viable alternative to SREIs.

The adaptive characteristics of unbonded FREIs are due to the combination of the unbonded application and lack of flexural rigidity of the fiber-reinforcement [7]. As lateral displacements are applied to the device, the isolator experiences *rollover*, shown in Fig. 2, or the loss of contact between the end sections of the isolator and the upper and lower supports. The resistance of the rollover section to lateral deformation is less than an equivalent section in simple shear. The size of the rollover section is also directly proportional to the displacement [22]. Thus, as the lateral displacement increases and the size of the rollover section increases, the lateral stiffness of the device decreases. This softening continues until the initially vertical faces of the isolator rotate 90° and contact the upper and lower supports preventing further rollover. The contact of the initially vertical faces and the supports is denoted as *full rollover*. Additional displacement beyond full rollover will result in a stiffening of the lateral response.

A comprehensive review of FREIs is available in the review by Van Engelen [2].

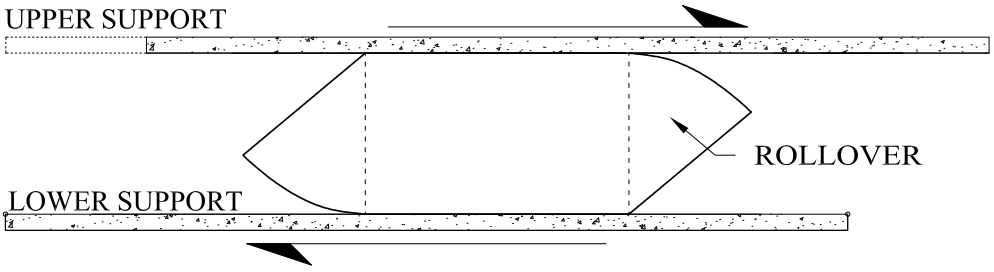

Fig. 2 - Rollover of an unbonded FREI due to lateral displacement

2.2 Strip Isolators

In addition to the potential for a reduction in the weight and cost of the isolation device, Kelly [3] also identified that FREIs could be cut to the desired size from larger pads. It was proposed that this, combined with the reduced weight, could enable the use of large strip isolators to provide uniform support along walls.

Such isolators could reduce the requirements of the load transfer system on-top of the isolation layer. Experimental investigations on strip or rectangular isolators have been conducted by numerous researchers [23–28]. Osgooei et al. [29] conducted time history analysis and confirmed the viability of using rectangular strip isolators on a masonry shear wall structure.

2.3 Lateral Coupling

Numerous numerical and experimental studies have investigated the lateral response of unbonded FREIs (e.g. [6,15,16,27,30–32]). Most studies apply the displacements aligned with the principal axes. However, the lateral response of unbonded FREIs may be different when the direction of the lateral load is not parallel to the principal axes (i.e. loading on both primary axes). The sensitivity to loading on a different axis, or lateral coupling, is an important design consideration. This has been investigated for square isolators, although it is notable that no studies consider the lateral coupling of rectangular unbonded FREIs.

Das et al. [8] investigated the lateral performance of square FREI specimens using three-dimensional finite element analysis (FEA) validated with experimental results. Two different directions of lateral displacement (i.e. along the *x*-axis and 45° to the *x*-axis) were considered to evaluate the effect of the loading direction. The results showed that the effective lateral stiffness at 45° was higher than the 0° loading direction at the same displacement. Osgooei et al. [9] conducted a similar study with three-dimensional FEA considering square unbonded FREIs having different aspect ratios and loaded at 0°, 15°, 30°, and 45° to the *x*-axis. The FEA was validated with experimental data of a square specimen loaded along the width of the isolator (i.e. 0°). It was observed that the effective lateral stiffness of the isolator increases as the loading direction is varied from 0° to 45°. Further, the results showed that as the aspect ratio decreases, the sensitivity of the lateral response of unbonded FREI to the loading directions increases. FEA results by [5] have shown that full rollover may also be influenced by the direction of loading.

Experimental testing conduct by Ngo et al. [10] at 0°, 15°, 30°, and 45° from the *x*-axis confirmed the FEA findings above [8,9]. The results showed that the effective lateral stiffness increases and the equivalent viscous damping decreases with changing the loading direction from 0° to 45° at all displacement amplitudes considered. In this study, FEA was also conducted to evaluate the effect of bidirectional loading on the response of unbonded FREIs by applying a constant displacement in one direction and cycles in the perpendicular directions. There was no significant coupling under the action of bidirectional loading. However, it was noted that the results were not comprehensive to reach definitive conclusions about the coupling behavior of the isolators and further studies are required.

An increase in effective lateral stiffness with increasing rotation from the principal axis (to an extent) is expected. As described above, the resistance of the rollover section is less than an equivalent volume in simple shear and the volume of rollover is proportional to the lateral displacement. As shown in Fig. 3, the area of rollover is greater in the 0° orientation than the 45° orientation, which is expected to result in a greater effective lateral stiffness for the 45° orientation, all else equal. In fact, only Ruano et al. [11] have observed contradictory results.

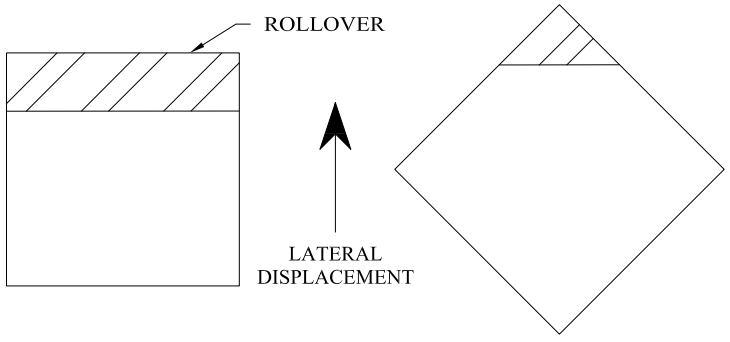

Fig. 3 – Plan view of identical square isolators with loading 0° and 45° to the principal axis at the same lateral displacement identifying the rollover area at the leading edge of the isolator.

3. Experimental Program

3.1 Specimen

Fig. 4 shows the specimen considered in this investigation and identifies the axis used to describe the experimental program. The specimen was manufactured as a large pad using a hot vulcanization process and subsequently cut to the desired size. The specimen was ¼ scale with a width of 100 mm (parallel to *x*-axis) and length of 60 mm (parallel to *y*-axis). The specimen was manufactured with seven layers of Shore A 40±5 durometer natural rubber with a specified loss factor of 0.1. The interior layers of natural rubber were nominally specified as 3.175 mm thick; the two exterior layers were half the thickness of the interior layers. Thus, the shape factor of the interior layers was S = 5.9 and S = 11.8 for the exterior layers. The total height of the bonded bearing was measured as approximately 20 mm with t_r = 19 mm. Plain-weave bidirectional carbon fiber with an areal weight of 190 g/m^2 was used as the reinforcement. The aspect ratio was R = 5.0 and 3.0 in the *x*- and *y*-directions, respectively. Thus, the specimen was designed to maintain lateral stability (i.e. a positive tangential stiffness) when displaced in the principal directions.

Fig. 4 - Fiber-reinforced elastomeric isolator specimen

3.2 Experimental Setup and Test Procedure

The experimental program was conducted in the Elastomers Laboratory at the Fiat Chrysler Canada Automotive Research and Development Centre located in Windsor, Ontario, Photography is strictly prohibited in the facility and photographs of experimental apparatus were not permitted. The apparatus was a six-degree of freedom (6DOF) system controlled by six actuators (1, 3, 2 in the *x*-, *y*-, and *z*-directions, respectively). Fig. 5 provides an approximate sketch of the apparatus. All loads are measured directly through a six-degree of freedom load cell. Displacements are measured with LVDTs at all actuators and corrected for geometric orientation during the test. Each actuator also contains a load cell for control and quality assurance purposes. The tests were conducted at room temperature (approximately 23°C).

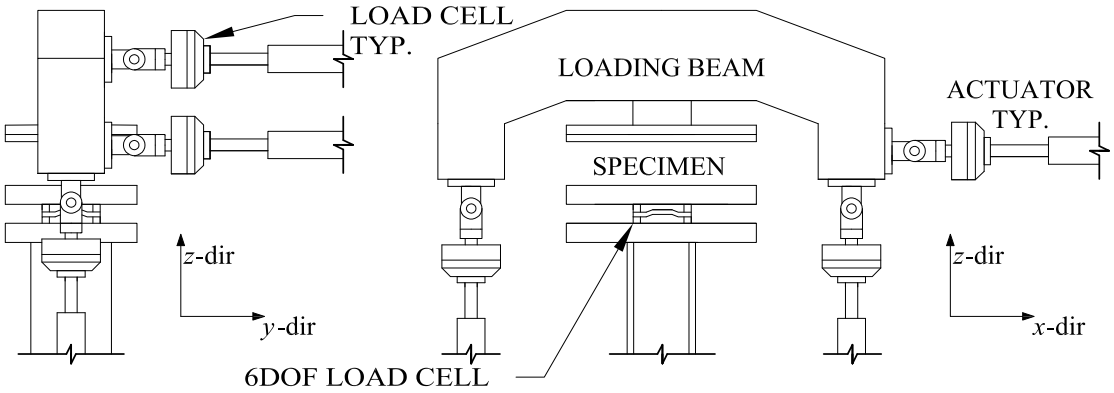

Fig. 5 - Approximate illustration of the experimental apparatus

All tests were conducted under an average vertical compressive stress of 3.0 MPa based on the total plan area. The scragged specimen was subjected to two lateral tests with intermittent vertical tests conducted to monitor the vertical stiffness for signs of deterioration or damage. In the first lateral test, six displacement amplitudes, up to u/t_r = 2.00, were considered in the *x*-direction. Fig. 6 shows the lateral time history used. The specimen was monotonically loaded in the *z*-direction up to the design average vertical compressive stress; the load was maintained during the experiment through load control. In the second lateral test, a lateral offset of u/t_r = 0.5 was applied in the *y*-direction and subsequently lateral cycles, identical to the first test, were applied in the *x*-direction. One sinusoidal cycle at each of the six displacement amplitudes were considered (i.e. u/t_r = 0.25, 0.5, 0.75, 1.00, 1.50 and 2.00). A seed time of five seconds was provided between the application of the vertical load and the lateral offset. The lateral cycles were conducted at a frequency of 1.25 Hz. The test program is summarized in Table 1.

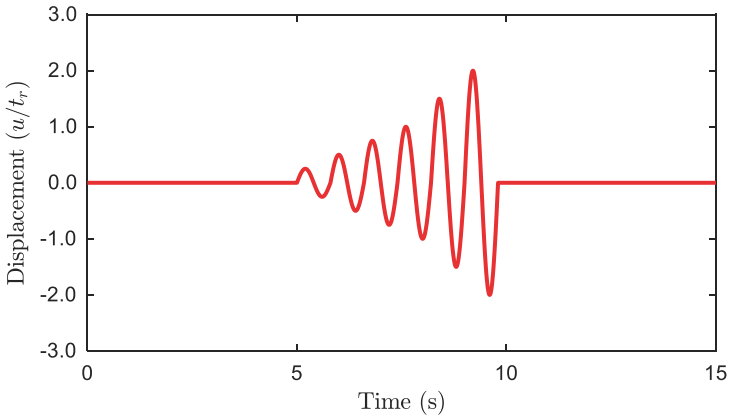

Fig. 6 – Lateral displacement time history

Table 1 – Experimental Program

Test	Amplitude (u/t_r)	
	x-dir	*y*-dir
Vertical 1	0	0
Lateral 1	0.25 to 2.0	0
Vertical 2	0	0
Lateral 2	0.25 to 2.0	0.5
Vertical 3	0	0

Vertical compressive tests were conducted between lateral tests. Each isolator was monotonically loaded to the design average vertical stress of 3.0 MPa. Three fully reversed sinusoidal cycles of ±20 % of the design average vertical stress were applied at a frequency of 0.1 Hz. A seed time of five seconds was allowed before and after the cycles. The specimen was then monotonically unloaded. The vertical loading was in accordance with procedures outlined in ISO 22762 [33].

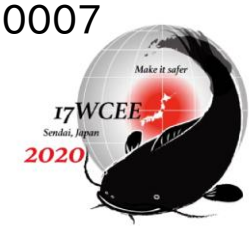

4. Results

4.1 Lateral Tests

As previously noted, photography in the Elastomers Laboratory at the Fiat Chrysler Canada Automotive Research and Development Centre was strictly prohibited. Thus, figures of the experiment program are not available.

4.1.1 Lateral Stiffness and Damping

The performance of the specimen is evaluated based on the effective lateral stiffness and the energy dissipation characteristics or the equivalent viscous damping. The effective lateral stiffness, k_L, was determined as [34]:

$$k_L = \frac{F_{L,\max} - F_{L,\min}}{u_{\max} - u_{\min}} \tag{1}$$

where $F_{L,max}$ and $F_{L,min}$ are the maximum and minimum lateral force observed over the cycle, and u_{max} and u_{min} are the maximum and minimum displacement observed over the same cycle, respectively.

The equivalent viscous damping, ζ_L, has been determined as [34]:

$$\zeta_L = \frac{2W}{\pi k_L \left(u_{\max} - u_{\min}\right)^2} \tag{2}$$

where W is the area enclosed within the hysteresis loops over the considered cycle.

Table 2 shows the experimentally obtained results for k_L, W, and ζ_L for each displacement amplitude considered. The table also shows the ratio of Test 2 to Test 1 for the respective parameters. In both cases, the specimen exhibits the characteristic softening and subsequent stiffening associated with unbonded FREIs, as shown in Fig. 7. The softening was observed up to the u/t_r = 1.50 cycle with a marginal increase in k_L at the u/t_r = 2.00 cycle. Note that the magnitude of the softening (approximately 30% decrease in k_L from the u/t_r = 0.25 cycle) is less than what could be observed due to the relatively high aspect ratio of R = 5.0. The value of ζ_L increases with increasing displacement amplitude in both cases. It is postulated that this is primarily due to the decrease in k_L. As expected, W also increases with increasing displacement amplitude.

Investigating the ratio of Test 2 to Test 1 illustrates that k_L inclusive of the offset is consistently lower than without the lateral offset. The decrease in k_L is initially 7% and decreases with increasing displacement amplitude to 1%. The equivalent viscous damping is initially 6% higher with the lateral offset and decreases to 4% lower at the maximum displacement amplitude. The ratio of the area enclosed within the hysteresis loops is relatively consistent and gradually decreases beginning at the u/t_r = 1.00 cycle to a maximum decrease of 5%.

Table 2 - Experimental results for the lateral properties as well as the ratio of Test 2 to Test 1

Cycle	k_L (kN/mm)			W (kN mm)			ζ_L (%)		
(u/t_r)	Test 1	Test 2	Ratio	Test 1	Test 2	Ratio	Test 1	Test 2	Ratio
0.25	0.225	0.208	0.93	1.4	1.4	0.98	4.5	4.7	1.06
0.50	0.198	0.187	0.94	5.4	5.3	0.98	4.9	5.0	1.04
0.75	0.179	0.171	0.95	11.8	11.6	0.98	5.2	5.3	1.03
1.00	0.164	0.158	0.96	20.9	20.3	0.97	5.6	5.7	1.01
1.50	0.154	0.149	0.97	50.0	47.9	0.96	6.4	6.3	0.99
2.00	0.163	0.161	0.99	102.9	98.0	0.95	7.0	6.7	0.96

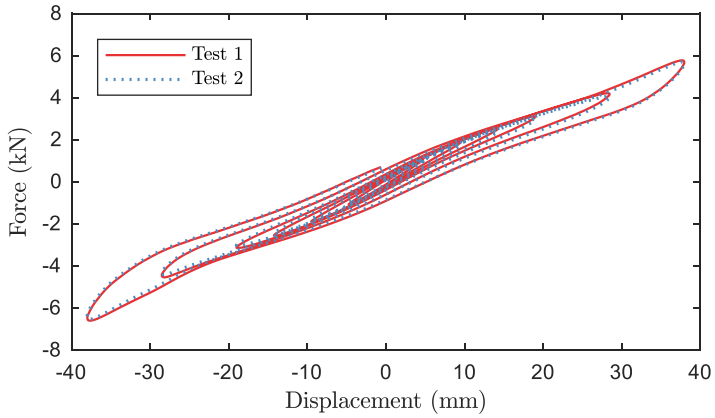

Fig. 7 – Force-displacement hysteresis loops for lateral Test 1 and Test 2

4.1.2 Residual displacement

During the second lateral test, it was observed that the isolator was visually displaced and retained a residual displacement in the negative *y*-direction (the initial displacement was in the positive *y*-direction). This observation suggests that the unbonded isolator experienced walking, or the gradual movement of the bearing, during cycles in the perpendicular direction. As the lateral offset was applied, the load initially increased to 1.47 kN in the *y*-direction, as shown in Fig. 8. During the seeding phase, the load gradually decreased to 1.30 kN at the start of the *x*-direction cycles due to the viscoelastic nature of elastomers. At the end of the cycles, the load was 0.88 kN which decreased to 0.83 kN at the start of the unloading ramp. The load at the end of the ramp was -0.65 kN.

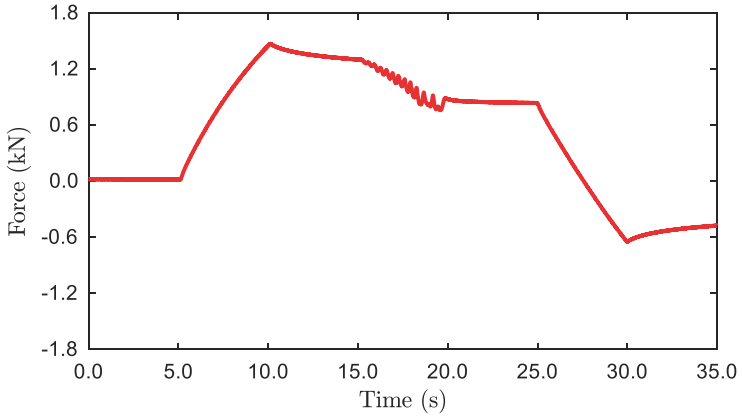

Fig. 8 – Time history for force in the *y*-direction during the second lateral test

4.2 Vertical Tests

The vertical tests were conducted to identify deterioration and damage between tests, if any. The evaluation is based on the vertical compression modulus, E_c, which is determined as:

$$E_c = \frac{k_v t_r}{A} \tag{3}$$

where A is the plan area of the isolator, and k_v is the vertical stiffness of the considered cycle defined as [34]:

$$k_v = \frac{F_{v,\max} - F_{v,\min}}{v_{\max} - v_{\min}} \tag{4}$$

where $F_{v,max}$ and $F_{v,min}$ are the maximum and minimum lateral force observed over the cycle, and v_{max} and v_{min} are the maximum and minimum displacement observed over the same cycle, respectively.

Fig. 9 shows the vertical load-displacement relationship obtained for the first vertical test. Table 3 provides the vertical compression modulus for the third cycle of each test as well as the percent change relative to the first test. The compression modulus was 77.0 MPa in the first test and decreased to 75.6 MPa in the second and third test (1.7% decrease). The magnitude of the decrease is relatively small and suggests that little-to-no damage was experienced by the specimen during the lateral tests. The isolator was also visually inspected between tests and no damage was observed. It is postulated that a portion of the decrease between the first and second vertical tests was due to additional scragging that may have occurred during the lateral test, or due to experimental error. The compression modulus of 77.0 MPa is many times greater than the elastic modulus of the elastomer alone, which is representative of the beneficial composite action provided by the reinforcement.

Table 3 – Vertical compression modulus results

Test	E_c (MPa)	% Change
Vertical 1	77.0	-
Vertical 2	75.6	-1.7%
Vertical 3	75.6	-1.7%

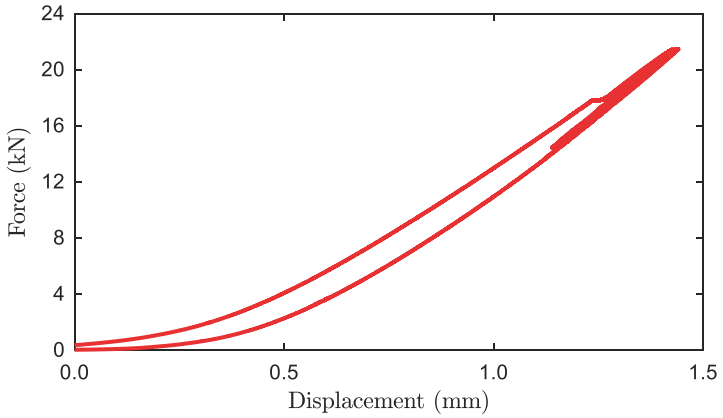

Fig. 9 – Force-displacement relationship from the first vertical test

5. Discussion

These preliminary results suggest that lateral coupling may occur in rectangular FREIs. It is expected that the lateral stiffness with an offset would be less than without an offset as the specimen is subjected to rollover along both principal axes. The magnitude of the difference in lateral stiffness is sufficiently high that additional investigation is required to determine the potential impact on the response of a structure with seismic excitation along both principal axes. The coupling effect, however, did not appear to have a pronounced effect on the energy dissipation, which was relatively unaffected during the low amplitude cycles. Note that the energy dissipation is more meaningful in this context as the equivalent viscous damping is a function of both the effective lateral stiffness as well as the area enclosed within the hysteresis loops. It is worth noting that the scragged bearing showed no signs of damage or deterioration during the test program

which is a testament to the possibility of manufacturing high-quality FREIs that can withstand many loading cycles.

Localized residual displacement has been observed in the end sections of the isolator due to rollover [35], or slip at high amplitude loading [2]. To the authors' best knowledge, this is the first observation of global residual displacements at relatively low displacement amplitudes. Walking, or the gradual movement of an unbonded bearing, is a natural phenomenon that can occur due to daily cycles from temperature variations [36]. It is postulated that the observed residual displacement was generated due to a similar phenomenon as walking, albeit accelerated due to the large amplitudes of the cycles. Due to safety considerations and restrictions on photography, the amplitude of the residual displacement was not directly determined. However, the force time history for the *y*-direction (see Fig. 8) shows that the change in load during the loading and unloading ramp was approximately equal at 1.47 kN. Based on this observation, if the stiffness is assumed to be constant, the change in load during the *x*-direction cycles (between 15 and 20 seconds) can be used to estimate the residual displacement. Following this approach, the residual displacement was approximately $u/t_r = 0.14$, or 28% of the *y*-direction offset.

Due to the residual displacement, the results presented herein should be interpreted acknowledging that the amplitude of the offset decreases with each subsequent cycle. This, in part, could be responsible for the increase in the k_L ratio with increasing lateral displacement shown in Table 2. Residual displacements are undesirable, but the current investigation considers only one specimen in specific loading conditions (e.g. vertical load) and of small scale. Furthermore, the condition of holding the displacement constant in one direction (i.e. the lateral offset) while cycling in the perpendicular direction is not representative of realistic earthquake loading. Thus, the susceptibility of unbonded FREIs to slip and residual displacements cannot be satisfactorily concluded based on this study. For low-cost applications, it may be found that the randomness of an earthquake effectively minimizes residual displacements to acceptable levels. Or, other variations of FREIs, such as including dowels or partially bonding the isolator to steel end-plates [25] may be implemented to prevent residual displacements. Comprehensive additional testing is required to further validate the observations in this paper as well as the potential for slip and residual displacements in unbonded FREIs.

6. Conclusion

Due to inherent non-linearities, unbonded fiber-reinforced elastomeric isolators may be more susceptible to lateral coupling than other traditional isolation devices. Although several preliminary studies have investigated the lateral coupling of square isolators, none have investigated the sensitivity of rectangular isolators. In this paper, an experimental program on a rectangular unbonded FREI isolator was presented. The experimental program was conducted with a six-degree of freedom apparatus that enabled a lateral offset to be applied and held perpendicular to the primary direction of lateral cycles. A comparison was conducted based on the effective lateral stiffness, equivalent viscous damping, and energy dissipation characteristics. Based on the results presented in this paper, which are limited to the specific specimen and loading conditions considered, rectangular unbonded FREIs do exhibit lateral coupling. However, the degree of coupling and the impact on the performance of a structure subjected to bi-directional lateral seismic excitation requires further investigation. During the test with an initial lateral offset, residual displacement was observed which was acknowledged to have impacted these results and conclusions.

These results are part of a larger experimental program being conducted by the authors which include additional tests with initial offsets, various vertical loads, testing the isolator at angles to the principal axis as well as circular bi-directional excitation. Lateral coupling is an important consideration that requires additional research. Although lateral coupling has been observed, the extent at which it should be accounted for in design needs to be determined and further investigated.

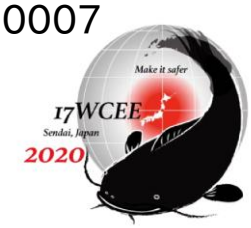

7. Acknowledgements

The assistance of Steve Hillman and other employees of the Fiat Chrysler Canada Automotive Research and Development Centre is greatly appreciated. The author acknowledges the support of the Natural Sciences and Engineering Research Council of Canada (NSERC) [funding reference number RGPIN-2019-03924].

8. References

[1] Clemente P (2017): Seismic isolation: past, present and the importance of SHM for the future. *Journal of Civil Structural Health Monitoring*, **7**(2), 217–231. DOI: 10.1007/s13349-017-0219-6.

[2] Van Engelen NC (2019): Fiber-reinforced elastomeric isolators: a review. *Soil Dynamics and Earthquake Engineering*, **125**, 105621. DOI: https://doi.org/10.1016/j.soildyn.2019.03.035.

[3] Kelly JM (1999): Analysis of fiber-reinforced elastomeric isolators. *Journal of Seismology and Earthquake Engineering*, **2**(1), 19–34.

[4] Toopchi-Nezhad H, Tait MJ, Drysdale RG (2011): Bonded versus unbonded strip fiber reinforced elastomeric isolators: Finite element analysis. *Composite Structures*, **93**(2), 850–859. DOI: 10.1016/j.compstruct.2010.07.009.

[5] Habieb AB, Milani G, Tavio T (2018): Two-step advanced numerical approach for the design of low-cost unbonded fiber reinforced elastomeric seismic isolation systems in new masonry buildings. *Engineering Failure Analysis*, **90**, 380–396. DOI: 10.1016/j.engfailanal.2018.04.002.

[6] Toopchi-Nezhad H, Drysdale RG, Tait MJ (2009): Parametric study on the response of stable unbonded-fiber reinforced elastomeric isolators (SU-FREIs). *Journal of Composite Materials*, **43**(15), 1569–1587. DOI: 10.1177/0021998308106322.

[7] Van Engelen NC, Tait MJ, Konstantinidis D (2015): Model of the shear behavior of unbonded fiber-reinforced elastomeric isolators. *Journal of Structural Engineering*, **141**(7), 04014169. DOI: 10.1061/(ASCE)ST.1943-541X.0001120.

[8] Das A, Dutta A, Deb SK (2015): Performance of fiber-reinforced elastomeric base isolators under cyclic excitation. *Structural Control and Health Monitoring*, **22**(2), 197–220. DOI: 10.1002/stc.1668.

[9] Osgooei PM, Tait MJ, Konstantinidis D (2014): Finite element analysis of unbonded square fiber-reinforced elastomeric isolators (FREIs) under lateral loading in different directions. *Composite Structure*, **113**, 164–173. DOI: 10.1016/j.compstruct.2014.02.033.

[10] Ngo T V, Deb SK, Dutta A (2018): Effect of Horizontal Loading Direction on Performance of Prototype Square Unbonded Fibre Reinforced Elastomeric Isolator. *Structural Control and Health Monitoring*, **25**(3), 1–18. DOI: 10.1002/stc.2112.

[11] Castillo Ruano P, Strauss A (2018): An experimental study on unbonded circular fiber reinforced elastomeric bearings. *Engineering Structures*, **177**, 72–84. DOI: 10.1016/j.engstruct.2018.09.062.

[12] Derham CJ, Kelly JM, Thomas AG (1985): Nonlinear natural rubber bearings for seismic isolation. *Nuclear Engineering and Design*, **84**, 417–428. DOI: 10.1016/0029-5493(85)90258-4.

[13] Thuyet VN, Deb SK, Dutta A (2018): Mitigation of seismic vulnerability of prototype low-rise masonry building using U-FREIs. *Journal of Performance of Constructed Facilities*, **32**(2), 04017136. DOI: 10.1061/(ASCE)CF.1943-5509.0001136.

[14] Crozier W, Stoker J, Martin V, Nordlin E (1974): A laboratory evaluation of full size elastomeric bridge bearing pads. *Technical Report CA-DOT-TL-6574-1-74-26*. Highway Research Report, Sacramento, CA.

[15] Toopchi-Nezhad H, Tait MJ, Drysdale RG (2008): Lateral response evaluation of fiber-reinforced neoprene seismic isolators utilized in an unbonded application. *Journal of Structural Engineering*, **134**(10), 1627–1637. DOI: 10.1061/(ASCE)0733-9445(2008)134:10(1627).

[16] Toopchi-Nezhad H, Tait MJ, Drysdale RG (2008): Testing and modeling of square carbon fiber-reinforced elastomeric seismic isolators. *Structural Control and Health Monitoring*, **15**(6), 876–900. DOI: 10.1002/stc.225.

[17] Strauss A, Apostolidi E, Zimmermann T, Gerhaher U, Dritsos S (2014): Experimental investigations of fiber and steel reinforced elastomeric bearings: Shear modulus and damping coefficient. *Engineering Structures*, **75**, 402–413. DOI: 10.1016/j.engstruct.2014.06.008.

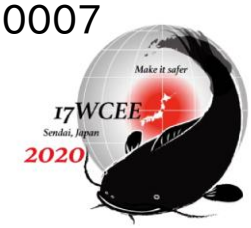

[18] Kang BS, Kang GJ, Moon BY (2003): Hole and lead plug effect on fiber reinforced elastomeric isolator for seismic isolation. *Journal of Materials Processing Technology*, **140**, 592–597. DOI: 10.1016/S0924-0136(03)00798-2.

[19] Bakhshi A, Jafari MH, Valadoost Tabrizi V (2014): Study on dynamic and mechanical characteristics of carbon fiber- and polyamide fiber-reinforced seismic isolators. *Materials and Structures*, **47**(3), 447–457. DOI: 10.1617/s11527-013-0071-z.

[20] Moon BY, Kang GJ, Kang BS, Kelly JM (2002): Design and manufacturing of fiber reinforced elastomeric isolator for seismic isolation. *Journal of Materials Processing Technology*, **130**–**131**, 145–150. DOI: 10.1016/S0924-0136(02)00713-6.

[21] Ashkezari GD, Aghakouchak AA, Kokabi M (2008): Design, manufacturing and evaluation of the performance of steel like fiber reinforced elastomeric seismic isolators. *Journal of Materials Processing Technology*, **197**(1–3), 140–150. DOI: 10.1016/j.jmatprotec.2007.06.023.

[22] Kelly JM, Konstantinidis D (2007): Low-cost seismic isolators for housing in highly-seismic developing countries. *10th World Conference on Seismic Isolation, Energy Dissipation and Active Vibrations Control of Structures*, Istanbul, Turkey.

[23] Van Engelen NC, Osgooei PM, Tait MJ, Konstantinidis D (2014): Experimental and finite element study on the compression properties of Modified Rectangular Fiber-Reinforced Elastomeric Isolators. *Engineering Structures*, **74**, 52–64. DOI: 10.1016/j.engstruct.2014.04.046.

[24] Osgooei PM, Van Engelen NC, Konstantinidis D, Tait MJ (2015): Experimental and finite element study on the lateral response of modified rectangular fiber-reinforced elastomeric isolators (MR-FREIs). *Engineering Structures*, **85**, 293–303. DOI: 10.1016/j.engstruct.2014.11.037.

[25] Van Engelen NC, Osgooei PM, Tait MJ, Konstantinidis D (2015): Partially bonded fiber-reinforced elastomeric isolators (PB-FREIs). *Structural Control and Health Monitoring*, **22**(3), 417–432. DOI: 10.1002/stc.1682.

[26] Kelly JM (2002): Seismic isolation systems for developing countries. *Earthquake Spectra*, **18**(3). 385–406. DOI: 10.1193/1.1503339.

[27] Van Engelen NC, Konstantinidis D, Tait MJ (2016): Structural and nonstructural performance of a seismically isolated building using stable unbonded fiber-reinforced elastomeric isolators. *Earthquake Engineering & Structural Dynamics*, **45**(3), 421–439. DOI: 10.1002/eqe.2665.

[28] Al-Anany YM, Van Engelen NC, Tait MJ (2017): Vertical and lateral behavior of unbonded fiber-reinforced elastomeric isolators. *Journal of Composites for Construction*, **21**(5), 04017019. DOI: 10.1061/(ASCE)CC.1943-5614.0000794.

[29] Osgooei PM, Tait MJ, Konstantinidis D (2016): Seismic isolation of a shear wall structure using rectangular fiber-reinforced elastomeric isolators. *Journal of Structural Engineering*, **142**(2), 04015116. DOI: 10.1061/(ASCE)ST.1943-541X.0001376.

[30] Toopchi-Nezhad H, Tait MJ, Drysdale RG (2012): Influence of thickness of individual elastomer layers (first shape factor) on the response of unbonded fiber-reinforced elastomeric bearings. *Journal of Composite Materials*, **47**, 3433–3450. DOI: 10.1177/0021998312466686.

[31] Kelly JM, Takhirov SM (2001): Analytical and Experimental Study of Fiber-Reinforced Elastomeric Isolators. Technical Report *PEER 2001/11*, Pacific Earthquake Engineering Research Center, Berkeley, USA.

[32] Kelly JM, Takhirov SM (2002): Analytical and Experimental Study of Fiber-Reinforced Strip Isolators. *Technical Report PEER 2002/11*, Pacific Earthquake Engineering Research Center, Berkeley, USA.

[33] ISO (2018): *Elastomeric seismic-protection isolators - Part 3: Applications for buildings - Specifications ISO 22762-3:2018*. Geneva: International Organization for Standardization.

[34] ISO (2018): *Elastomeric seismic-protection isolators - Part 1: Test methods ISO 22762-1:2018*. Geneva: International Organization for Standardization.

[35] Russo G, Pauletta M (2013): Sliding instability of fiber-reinforced elastomeric isolators in unbonded applications. *Engineering Structures*, **48**, 70–80. DOI: 10.1016/j.engstruct.2012.08.031.

[36] McDonald J, Heymsfield E, Avent RR (2000): Slippage of neoprene bridge bearings. *Journal of Bridge Engineering*, **5**(3), 216–223.

